Accepted Manuscript

Enhanced photocatalytic oxidation of SO_2 on TiO_2 surface by Na_2CO_3 modification

Haiming Wang, Changfu You, Zhongchao Tan

PII: S1385-8947(18)30942-2
DOI: https://doi.org/10.1016/j.cej.2018.05.128
Reference: CEJ 19144

To appear in: *Chemical Engineering Journal*

Received Date: 7 March 2018
Revised Date: 11 May 2018
Accepted Date: 21 May 2018

Please cite this article as: H. Wang, C. You, Z. Tan, Enhanced photocatalytic oxidation of SO_2 on TiO_2 surface by Na_2CO_3 modification, *Chemical Engineering Journal* (2018), doi: https://doi.org/10.1016/j.cej.2018.05.128

Enhanced photocatalytic oxidation of SO_2 on TiO_2 surface by Na_2CO_3 modification

Haiming Wang[1,2], Changfu You[1,3]*, Zhongchao Tan[2,3]*

1. Key Laboratory for Thermal Science and Power Engineering of the Ministry of Education, Department of Energy and Power Engineering, Tsinghua University, Beijing 100084, China
2. Department of Mechanical and Mechatronics Engineering, University of Waterloo, Ontario, Canada N2L 3G1
3. Tsinghua University – University of Waterloo Joint Research Centre for Micro/Nano Energy & Environment Technologies, Tsinghua University, Beijing, China 100084

*Corresponding authors:
Changfu You: youcf@tsinghua.edu.cn
And
Zhongchao Tan: tanz@uwaterloo.ca

Abstract: The effects of Na_2CO_3 on the photocatalytic oxidation (PCO) of SO_2 with UV irradiated TiO_2 (P25) were studied using a fixed bed reactor. Na_2CO_3 was loaded onto P25 using a wet coating method. The PCO efficiency for SO_2 with P25 was enhanced by 1.6 and 10.6 times using 0.05M and 0.2M Na_2CO_3 modified P25, respectively. The enhancement of the photocatalytic activity of P25 by Na_2CO_3 was observed only with the presence of water vapor. Low temperature (113K) electron spinning resonance (ESR) analysis showed that Na_2CO_3 promoted the photoinduced electron-hole separation by trapping valance band holes and forming carbonate radicals ($CO_3^{\bullet-}$). The ESR spin trapping analyses showed a remarkable increase in the intensity of [DMPO-OH] adducts with the addition of Na_2CO_3. This increase phenomena indicates that more reactive species were formed on the P25 surface. The deposited Na_2CO_3 inhibited the recombination of electron-hole pairs and promoted the generation of hydroxyl radicals (•OH), most likely through the photo-reduction of O_2 adsorbed by the conduction band electrons. The generated •OH radicals reacted with SO_2 rapidly and improved the PCO effectiveness of P25.

Keywords: Photocatalytic oxidation, Titanium dioxide, Sodium carbonate, Sulfur dioxide, Electron spinning resonance

1. Introduction

Photocatalysis, as an efficient redox technique, has attracted considerable attention in air cleaning and water purification applications [1-3]. Titanium dioxide (TiO_2) based catalysts are the most widely tested photocatalyst for this purpose [1, 4]. The photoinduced electron-hole pairs under UV irradiation on TiO_2 surface can be transferred to the catalyst surface to initiate redox; they also undergo recombination to release heat. The recombination lowers the quantum efficiency of the photocatalytic reaction and limits the activity of TiO_2 [5, 6].

A number of surface modification strategies have been developed in the past few decades to improve the separation of photoinduced electron-hole pairs before their recombination [7, 8]. For example, the deposition of noble metals such as Pt [9] and Au [10, 11] enhanced the photocatalytic activity by increasing the formation rate of electron-hole pairs and/or accelerating the transfer of the pairs to the catalyst interface. Modifying TiO_2 with carbon-based nanomaterials such as carbon nanotube [12] and graphene [13] can also increase the electron transfer rate and the adsorption ability of the catalysts. The effects of inorganic anions including Fluoride (F^-), sulfate (SO_4^{2-}), and phosphate (PO_4^{3-}) on the photocatalytic activity of TiO_2 were also investigated for the decomposition of contaminants. These anions were able to alter the pathways of charge transfer [7] through enhanced hole transfer [14], and/or improved generation of free hydroxyl groups [15], surface stability and surface acidity [16].

Carbonate (CO_3^{2-}) is a common and pervasive species in both aqueous and solid phases. However, there are limited studies on the effects of CO_3^{2-} on the photocatalytic activity of TiO_2 for environmental remediation [17]. Carbonate salts, mostly sodium carbonate, reportedly play a different role in the photocatalytic oxidation of contaminants in liquid with TiO_2 suspensions. The addition of Na_2CO_3 has been found to improve the PCO of aniline and phenol.[17, 18] The proposed

enhancement mechanisms depend on the contaminants. For the PCO of phenol, the formation of $CO_3^{\bullet-}$ from the hole oxidation of carbonate enhanced the hole transfer from TiO_2 to phenol [17]. An increased number of adsorption sites on TiO_2 surface and the combination of $CO_3^{\bullet-}$ and •OH were considered the main reasons behind the improvement of the photocatalytic degradation of aniline [18]. Sayama et al. [19, 20] found that the overall water splitting on Pt/TiO_2 was expedited by the addition of Na_2CO_3. It promoted the formation of peroxycarbonate via the reaction between carbonate anions and photoinduced holes on the TiO_2 surface.

On the other hand, the inhibition effect of carbonate anions on PCO was also reported in TiO_2 suspensions. For the PCO of dichloroethane (DCE), the competitive adsorption of DCE and anions on the TiO_2 surface decreased the decomposition rate of DCE [21]. Even though the adsorption of acid red 88 (AR) was promoted by the addition of bicarbonate anions (HCO_3^-), the detrimental effects on the PCO of AR with TiO_2 were attributed to possible scavenging of hydroxyl radicals (•OH) to form carbonate radicals ($CO_3^{\bullet-}$), which were less active than •OH [22]. Both the aforementioned drawbacks were observed when Bouanimba et. al. [23] used P25 suspensions to degrade methyl orange (MO) mixed with $NaHCO_3$ or Na_2CO_3.

Therefore, the effects of carbonate salts on TiO_2 photocatalysis could be system dependent. To our best knowledge, the effects of carbonate salts on the photocatalytic activity have mostly been tested for the PCO of aqueous contaminants using TiO_2 suspensions. There are few reports for the effects of carbonate on the PCO of gaseous pollutants with TiO_2 particles.

In this work, the gaseous pollutant of concern is sulfur dioxide (SO_2). SO_2 is largely emitted from the combustion of sulfur-containing fuels. It is a common air pollutant that negatively impacts the environment and public health [24]. SO_2 in the atmosphere

can be oxidized by photocatalysts (contained in mineral dusts) into sulfuric acid and/or sulfate, which cause acid rain and secondary aerosol particles [25-27].

Photocatalytic technology has been developed recently to treat SO_2 in indoor air [28, 29] and industrial flue gases [30-35]. The PCO of SO_2 is caused by the oxidative species generated on UV irradiated TiO_2 surfaces. The hydroxyl radicals (•OH) and superoxide radicals ($O_2^{\bullet-}$) are two well known, important oxidative radicals that trigger the redox reactions [4]. Several researchers reported the PCO of SO_2 with these radicals on TiO_2 surfaces [30, 36]. The possible reaction mechanism has been proposed for the oxidation process:

$$SO_2(ads) + 2{\bullet}OH \rightarrow SO_3(ads) + H_2O \quad (1)$$

$$SO_2(ads) + {\bullet}O_2^- \rightarrow SO_3(ads) + O^- \quad (2)$$

$$SO_3^{2-} + 2{\bullet}OH \rightarrow SO_4^{2-} + H_2O \quad (3)$$

$$SO_3(ads) + H_2O(ads) \rightarrow H_2SO_4(ads) \quad (4)$$

Researchers have tried to modify TiO_2 to improve the PCO efficiency of SO_2 aiming at industrial applications. The modification methods include supporting TiO_2 with activated carbon [28], multi-walled carbon nanotubes [37], electro-spun nanofibers [30, 35], and doping TiO_2 with Cu [37], Mn [31], and N [32]. Carbonates are commonly present in the atmosphere and flue gas, and may deposit on the catalyst surface and affect the PCO process. However, their effects on the PCO of SO_2 and the reaction mechanisms are not available in literature. To understand their possible roles in the PCO of SO_2, it is worth investigating the photocatalytic performance of TiO_2 in the presence of carbonate salts.

In this study, therefore, the effects of Na_2CO_3 on the PCO of SO_2 by P25-TiO_2 were investigated using a homemade fixed bed reactor. The performances of catalysts modified with NaCl, $NaNO_3$, Na_2SO_4, NaOH, and $NaHCO_3$ were also compared with Na_2CO_3. Different characterization techniques, including X-ray photoelectron

spectroscopy (XPS), X-ray Diffraction (XRD), and UV-Vis diffuse reflectance spectroscopy (UV-Vis DRS), were used to characterize the morphology of TiO_2 before and after the catalyst modification and the photocatalytic reaction. Furthermore, low temperature (113K) electron spinning resonance (ESR) and ESR spin trapping methods were used to understand the possible mechanisms of the enhanced photocatalytic activity with respect to Na_2CO_3.

2. Experimental

2.1. Sample preparation

P25-TiO_2 (Evonik) was used as the basic photocatalyst in this study. Gas cylinders and chemical reagents were purchased from Air Liquid and Sinopharm Chemical Reagent, Beijing, China, respectively, unless stated otherwise. The photocatalyst was immobilized on inert glass beads, of which the sizes are in the range of 0.4-0.5 mm in diameter. It is deemed to avoid the large pressure drops caused by packing P25 nanoparticles in the fixed bed reactor. The detailed procedure was described elsewhere [34] and briefly summarized as follow. The glass beads were first washed using hydrofluoric acid and then immersed in P25 suspensions by continuous stirring for 30 min. Glass beads loaded with P25 were dried at 80 ℃ for 2 hr followed by calcination in a muffle furnace at 400 ℃ for 3 hr. The coating weight of TiO_2 was approximately 20mg/g glass beads.

Photocatalysts modified with carbonate salts were prepared by washing the immobilized P25 with corresponding solution of different concentrations (0.005 to 0.2 mol/L). For a typical procedure, 3±0.01 g of glass-beads-P25 composites was impregnated in 50 ml of solution for 30 min. After separation from liquid, the wet composite catalyst particles were dried at 105℃ in an oven for 6 hr. The resultant samples were then labeled in the format of P25-A-B, where A and B represent the concentration of solution and the name of chemical reagent, respectively.

2.2. Photocatalytic activity measurement

The photocatalysts were tested for their effects on PCO of SO_2 using a homemade fixed bed reactor. As shown in Figure 1, the reactor was surrounded by four UV lamps providing an intensity of 3 mW/cm^2 at the peak wavelength of 365 nm. The UV intensity was measured by a UV light meter ST513 (Sentry Optronics Corp.). More information about the reactor can be found in literature [34].

Comparative tests were conducted following the same procedure under identical conditions for P25 before and after modification with Na_2CO_3. In each test, simulated flue gas, containing 40 ppm SO_2, 5 vol% O_2, and 2.9 vol% H_2O mixed with nitrogen the balance gas, passed through the reactor at a flow rate of 100 sccm. The reaction temperature was maintained at 60±1℃ using a temperature controller (Shimaden, Japan). Three grams (3±0.01 g) of photocatalyst was packed into the reactor with a height of 160 mm. The corresponding superficial residence time was 1.2 s.

SO_2 concentration in the gas stream was monitored by an online gas analyzer (Model 43C, Thermo Scientific). The inlet SO_2 concentration was taken for 10 minutes of stable reading prior to the onset of the test. Then the gas flow was introduced into the catalyst bed via three-way valves. The adsorption of SO_2 without UV light was firstly conducted until the adsorption reached its breakthrough. Afterward, the UV irradiation was activated to trigger the photocatalytic oxidation. The variation of the outlet SO_2 concentration was recorded every minute in the test. The performance of the catalyst is quantified by SO_2 penetration rate (P), which is defined as the ratio of outlet (C_{out}) to inlet SO_2 concentrations (C_{in}):

$$P = \frac{C_{out}}{C_{in}} \tag{5}$$

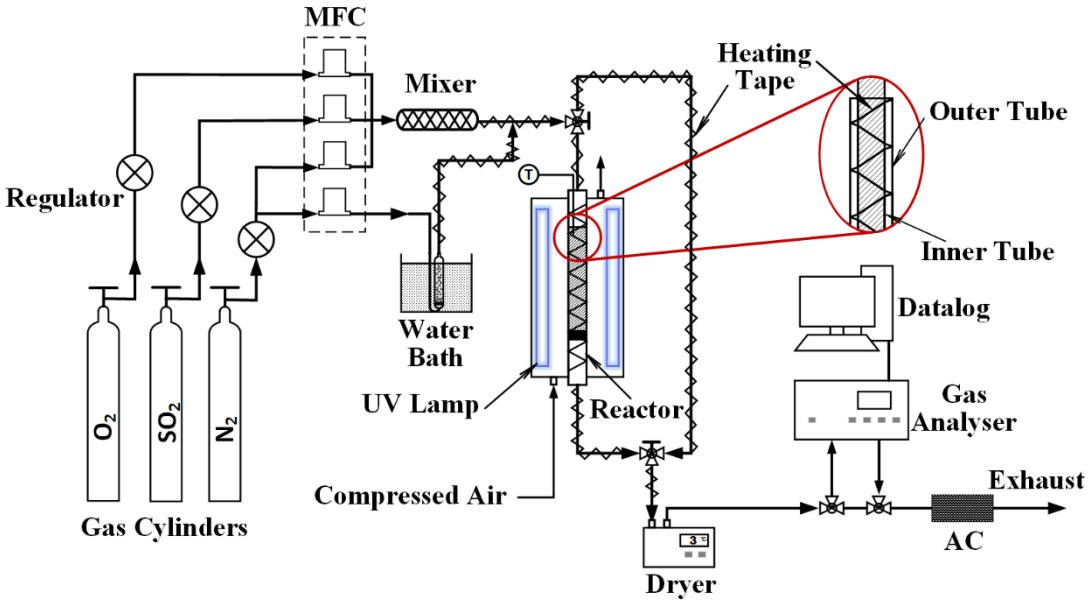

Figure 1. Diagram of the experimental setup

The Na_2CO_3 modification process could introduce different factors which may affect the photocatalytic activity of P25. They include enhanced adsorption of SO_2 (due to the reaction between the deposited Na_2CO_3 and SO_2), deposited sodion (Na^+), deposited carbonate/bicarbonate ions (CO_3^{2-}/ HCO_3^-), and hydroxyl groups (OH^-) in the Na_2CO_3 solution. To quantify their relative importance, the following tests were also conducted following the same procedure mentioned above.

1) A blank test: The inert glass beads without P25 coated with Na_2CO_3 by soaking in Na_2CO_3 solution (0.2 M) and tested for PCO of SO_2.
2) Tests for P25 modified with different sodium salts including NaCl, $NaNO_3$, and Na_2SO_4. The results were compared with that of P25 modified with Na_2CO_3 to study the effects of Na^+ on the PCO of SO_2. The concentrations of all the above sodium salts were 0.2M.
3) Tests for P25 modified with 0.01M NaOH. There are hydroxyl groups in Na_2CO_3 solution, which may deposit on P25 surface and affect its surface activity. 0.01M NaOH solution (pH=12) was used to replace 0.2M Na_2CO_3 (pH=11.8). The goal

was to study the possible influences of OH^- on the performance of P25 while eliminating the effect of CO_3^{2-}.

4) Tests for P25 modified with 0.2M $NaHCO_3$. Both CO_3^{2-} and HCO_3^- exist in Na_2CO_3 solutions. They deposit on P25 surface and may affect the PCO of SO_2 too. It is necessary to investigate the roles of HCO_3^- and CO_3^{2-} in the PCO performance using P25 modified by Na_2CO_3.

2.3. Characterization of photocatalysts

The samples were characterized using multiple equipment to investigate the mechanisms underlying the effects of Na_2CO_3 modification on the photocatalytic activity of P25. The crystal phase of glass beads, P25, and modified catalyst composites were characterized by XRD to identify the change in the crystal phase of TiO_2 resulted from the modification. The XRD analyses were conducted using D/max2550HB+/PC diffractometer with Cu-Kα radiation (λ=0.15418 nm) in continuous scan mode with a step size of 0.02° in the 2θ range of 10° to 80°.

XPS study was carried out to identify the surface speciation and possible reaction products on the P25 surface before and after the PCO of SO_2. It was conducted using the Escalab 250Xi (Thermo Scientific) with monochromatic radiation from Al Kα source at hυ=1486.6 eV. The binding energy of C1s, which is 284.8 eV, was taken as an internal energy reference for calibration in all experiments.

UV-Vis DRS of catalysts was recorded on a UV-Vis-NIR spectrophotometer UV3600 (Shimadzu, Japan) for wavelength from 200 to 800 nm. The corresponding results were used to analyze the UV-Vis irradiation acceptance. They can also be used for the calculation of the band gaps of the photocatalysts.

Electron Spin Resonance (ESR) technology offers a great potential to trap short-lived

radical species on the photo-irradiated TiO_2 surface. This information can be useful to the elucidation of photo-induced surface reactions. In this study, therefore, ESR spectra of P25 modified with different reagents were analyzed using JES-FA200 ESR Spectrometer (JEOL, Japan) operating in X-band at a microwave frequency of 9.06 GHz. The UV irradiation was introduced by an ultrahigh-pressure mercury UV lamp (Ushio SX-UI502HQ, Ushio Inc.) with an intensity of 50 mW/cm^2. Mn^{2+} was used as an internal standard (g_3=2.0345, g_4=1.9804) to calibrate the sample spectra. The other ESR spectrometry parameters are listed as follows:

- Power: 0.998 mW
- Modulation frequency: 100 kHz
- Modulation width: 0.1 mT
- Sweep width: ~10mT
- Sweep time: 1-3 min
- Temperature: 113K (For ESR spectra of solid samples)
- Concentration of P25: 10 g/L (For ESR spin trap).

For each solid test, 50 mg of catalyst was loaded into the ESR. With UV irradiation the ESR recorded the signals of the surface trapped holes and electrons. The ESR spin trapping was also conducted for P25 suspensions at room temperature with 50 mmol/L 5,5-dimethyl pyrroline N-oxide (DMPO, Sigma Aldrich) as the trapping agent. DMPO can trap hydroxyl radical (•OH) produced on the surface of irradiated TiO_2 to form paramagnetic adduct [DMPO-OH], which can be identified by ESR.

3. Results and Discussion

3.1. Photocatalytic oxidation of SO_2 on bare P25

Figure 2 shows the variation of SO_2 penetration rate vs. time on stream (TOS) for P25 without modification. The adsorption breakthrough time and reaction breakthrough time were denoted as t_{ab} and t_{rb}, respectively. SO_2 outlet concentration decreased dramatically to zero due to the strong adsorption of TiO_2 in dark. The UV lamps were

then turned on after the adsorption breakthrough of the catalyst bed, when the photocatalytic reaction took place on the catalysts surface. The corresponding C_{out} dropped sharply again to zero. However, after a relatively short duration of high-efficiency reaction, the efficiency of the photo-reaction began to decline as indicated by the rising SO_2 penetration rate. This is the result of the adsorption of the reaction products which covered the surface active sites and deactivated the catalyst [30, 34].

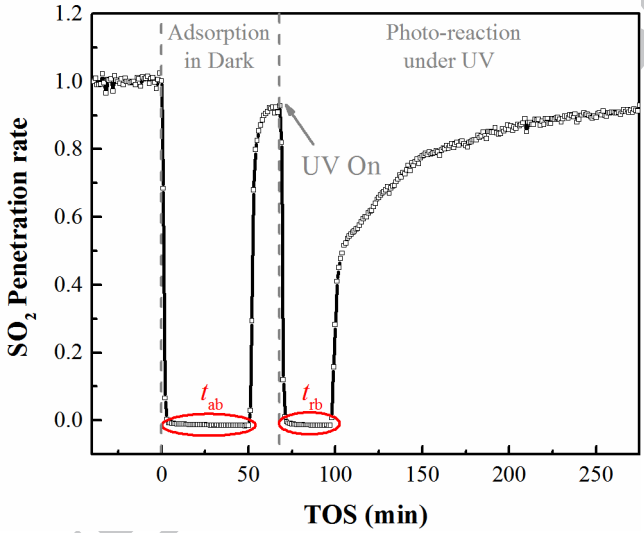

Figure 2. Change of SO_2 penetration rate vs. TOS for P25

Figure 3 shows the high resolution XPS spectra of S2p and Ti2p before and after the reactions. No signals of sulfur compounds were observed on the fresh P25 catalyst (Figure 3A (a)). After the SO_2 adsorption in dark, a strong signal was observed, which can be subdivided into the characteristic S2p doublet. The S2p doublet of $S2p_{3/2}$ and $S2p_{1/2}$ with the binding energies of 167.8 eV and 169.0 eV, respectively, was assigned to the surface bounded sulfite/SO_2 [38]. The binding energies of the doublet shifted to higher values after UV irradiation (Figure 3A (c)), which can be assigned to the sulfate species such as SO_4^{2-} (H_2SO_4) and/or SO_3 [39], indicating the oxidation of the SO_2 or sulfite on the irradiated catalyst surface. Similar shifting was observed in terms of the binding energy of Ti2p spectra after the photocatalytic oxidation of SO_2. The

adsorption of SO_2 had negligible effect on the binding energy of the fresh P25 sample, as shown in Figure 3B (b). Nevertheless, after UV irradiation, the PCO products adsorbed on P25 surface caused the increment of the binding energy of Ti2p from the original 458.5 eV to 458.9 eV (Figure 3B (c)).

As seen in Figure 3, $S_{(VI)}$ was formed on the irradiated P25 surface. To further determine the species on the catalyst surface, the fresh P25 sample was washed with 0.1 M H_2SO_4 followed by drying at 105 ℃ for 6 hr. It was next tested to check the influences of the accumulated sulfate ions. The corresponding high resolution XPS spectra are shown in Figure 3 (d). It was found that the samples washed with H_2SO_4 showed the same S2p doublet as on the UV irradiated catalyst surface (Figure 3A (c) and (d)). The accumulated H_2SO_4/SO_4^{2-} also caused the same shifting in binding energy of Ti2p (Figure 3B (c) and (d)). In the present study, the flue gas temperature was maintained at 60℃, and the water content was 2.9 vol% which is three orders of magnitudes greater than the concentration of SO_2. It was reported that over 95% of the SO_3 was converted into H_2SO_4 at the temperature below 200℃ with the presence of water vapor [40]. As such, we can conclude that the PCO products of SO_2 existed mainly in the form of H_2SO_4/SO_4^{2-} instead of SO_3. The deactivated catalyst can simply be regenerated partially as described in previous studies due to the high solubility of the PCO products [30, 34].

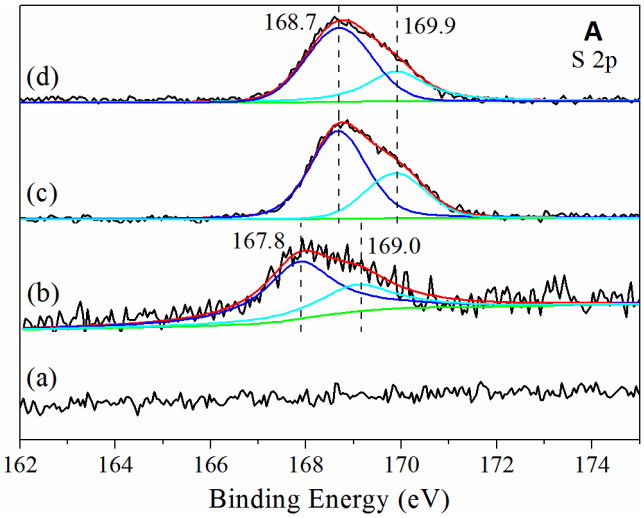

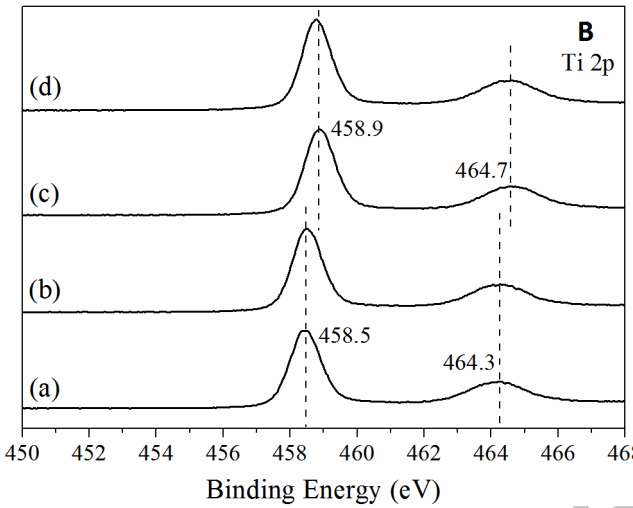

Figure 3. High resolution XPS spectra for P25, A: S2p, and B: Ti2p. (a) fresh P25, (b) after the SO_2 adsorption in dark, (c) after PCO, (d) after washing by 0.1 M H_2SO_4

3.2. Effects of Na_2CO_3 on the PCO of SO_2

The blank test results are shown in Figure 4. It indicates that the Na_2CO_3 itself cannot react with SO_2 under UV-irradiation after the adsorption breakthrough. Without immobilizing P25, glass beads exhibited very weak adsorption ability for SO_2. UV irradiation caused a slight decrease in the outlet SO_2 concentration, which was negligible compared to the photocatalytic ability of P25 shown in Figure 2. After doping with Na_2CO_3, the accumulated Na_2CO_3 on the surfaces of the glass beads can react with SO_2 to produce Na_2SO_3/$NaHSO_3$. They changed the physisorption on glass beads to chemisorption, which enhanced the SO_2 adsorption. However, the photocatalytic activity was similar to that of the bare glass beads; this indicates that Na_2CO_3 itself did not have the ability to oxidize SO_2 through photo-reaction. The enhancement of the PCO ability observed for the P25 modified with Na_2CO_3 in the following experiments should mainly be attributed to the interaction between Na_2CO_3 and TiO_2 surface. This will be discussed in detail below.

Worth noting is that the chemisorption of SO_2 on surface deposited Na_2CO_3 can possibly cause the loss of the effective component CO_3^{2-}. The gaseous CO_2 can be produced by the reaction between SO_2 and Na_2CO_3. However, not all of the products

are released from the surface of TiO_2. According to a recent study[27], the adsorption uptake of CO_2 on TiO_2 (~1.5×10^{13} molecules/cm^2) is of the same magnitude as that of SO_2 on TiO_2 (~5.0×10^{13} molecules/cm^2). Thus the generated CO_2 are likely adsorbed onto TiO_2 even though the existence of SO_2 would decrease the adsorption ability of CO_2 on TiO_2[41]. The adsorbed CO_2 on TiO_2 has shown the formation of carbonate and bicarbonate species as reported by other researchers [27, 41, 42]. In addition, the surface deposited Na_2CO_3, especially the Na_2CO_3 attached right next to the surface of the TiO_2, will not react with SO_2 completely, which can be inferred from the low efficiency after the adsorption breakthrough. To confirm the existence of the surface carbonate/bicarbonate species, the XPS analysis was conducted to characterize the Na_2CO_3 modified catalyst before and after the SO_2 adsorption (shown in Figure S1). After the modification, the high resolution XPS spectrum of C1s presents a peak with an increased intensity at the binding energy of 289.3 eV, which is assigned to carbonate species (Na_2CO_3 in [43]). After SO_2 adsorption, the peak intensity decreases slightly yet remaining much stronger than the catalyst before modification.

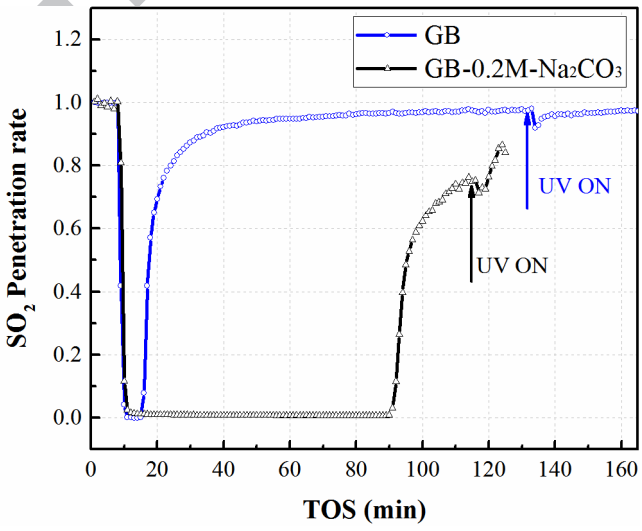

Figure 4. Blank test results for original glass beads (GB) and those washed with 0.2M-Na_2CO_3

Figure 5 shows the SO_2 penetration rate over time with P25 modified by Na_2CO_3 of

different concentrations. The photocatalytic ability of P25 was improved dramatically after being modified with 0.2M Na_2CO_3. The improvement rate, however, gradually decreased with the decreasing concentration of Na_2CO_3. Not much improvement was found when P25 was modified with 0.005M Na_2CO_3. As Table 1 shows, the photocatalytic reaction breakthrough time t_{rb} increased by 1.04, 1.64, 4.96 and 10.6 times when the catalysts were modified with 0.005, 0.05, 0.1 and 0.2 M Na_2CO_3, respectively. The PCO capacity of SO_2 with bare P25 under UV irradiation was about 5.8 mg SO_2/g TiO_2, while it could be as high as 61.5 (mg SO_2/g TiO_2) after the modification with 0.2 M Na_2CO_3. As stated, the mechanisms of Na_2CO_3 modification could be attributed to the adsorption enhancement of SO_2 (as observed in Figure 4), and Na^+, CO_3^{2-}/ HCO_3^- and OH^- in the used Na_2CO_3 solution. Their effects on the enhancement of P25 activity are discussed as follows.

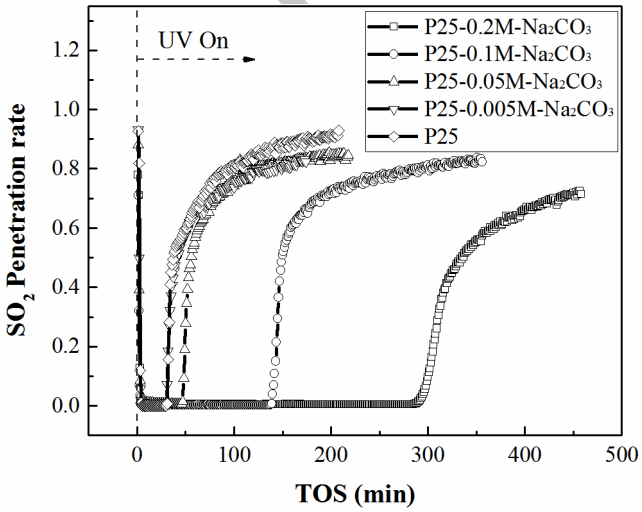

Figure 5. PCO performances of the catalysts modified with Na_2CO_3 of different concentrations

Table 1 shows the adsorption breakthrough time (t_{ab}) for bare P25 and P25 modified with different salts. It can been seen that the t_{ab} was increased from 50 min for bare P25 to 570 min for P25-0.2M-Na_2CO_3. This adsorption improvement resulted from the reaction between the deposited Na_2CO_3 and SO_2 as discussed in the blank test

results. The PCO of gaseous SO_2 on the surface of TiO_2 is a heterogeneous catalytic reaction. SO_2 was firstly adsorbed on the catalyst surface for the reaction to take place. Therefore, it is reasonable to say that the improved photocatalytic activity could be attributed to the enhanced adsorption ability of the catalyst. However, the improvement for the photocatalytic activity of P25 cannot be explained solely by the enhanced adsorption ability of the catalyst.

Figure 6 shows the comparison of the adsorption breakthrough time (t_{ab}) with the photo-reaction breakthrough time (t_{rb}). It shows that t_{ab} increased almost linearly with the concentration of Na_2CO_3, while t_{rb} increased slowly at low Na_2CO_3 concentration (<0.05 M) and then increased much faster at higher concentrations. In addition, $NaHCO_3$ was used to modify P25 in this study, and it could also improve the chemisorption of SO_2. The performance of P25-0.2M-$NaHCO_3$ was compared to that of P25-0.1M-Na_2CO_3 (same Na^+ concentration) and that of P25-0.2M-Na_2CO_3 (same carbon species concentration). Even though the t_{ab} of P25-0.2M-$NaHCO_3$ (488 min) was much longer than that of P25-0.1M-Na_2CO_3 (335 min), the photocatalytic activity of the former was about two times less (see Table 1). If the carbon species concentration remained unchanged (i.e., using 0.2M Na_2CO_3 modified P25), the photo-reaction capability could be four times higher than that treated using 0.2M $NaHCO_3$. As a result, catalyst modification with Na_2CO_3 could enhance not only the adsorption ability, but also the photocatalytic activity of TiO_2 under UV-irradiation.

Table 1. Breakthrough time and SO_2 dealing capacity for P25 modified by different reagents

Reagents	Concentration (mol/L)	pH*	t_{ab} (min)	t_{rb} (min)	Capacity** (mg SO_2/g TiO_2)
Bare P25	--	--	50	28	5.8
Na_2CO_3	0.005	10.9	55	29	5.8
	0.05	11.5	251	46	9.0
	0.1	11.6	335	139	26.5
	0.2	11.8	570	297	61.5
$NaHCO_3$	0.2	--	488	73	13.3
NaCl	0.2	--	21	20	3.9
$NaNO_3$	0.2	--	18	15	3.0
Na_2SO_4	0.2	--	18	20	3.9
NaOH	0.01	12	45	23	4.7

*: The theoretical pH value calculated by the proton balance equation

**: The photocatalytic oxidation capacity of SO_2 per gram TiO_2 before the photo-reaction breakthrough (with almost 100% removal efficiency of SO_2)

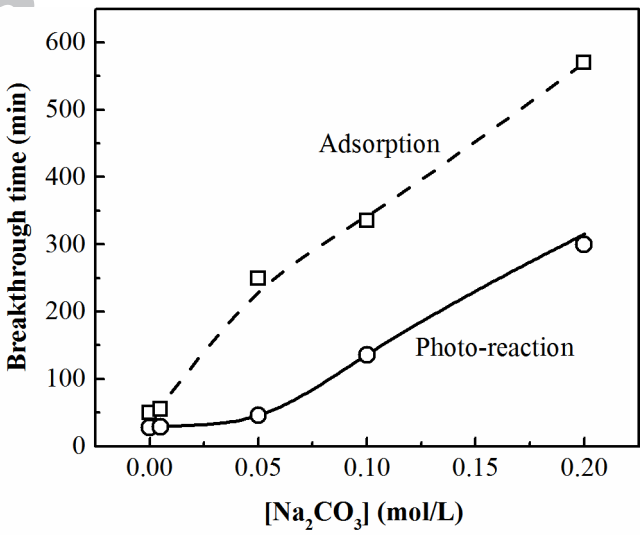

Figure 6. The adsorption and photo-reaction breakthrough times for P25 modified with different concentrations of Na_2CO_3 solution

The deposition of Na^+ on catalyst surface did not contribute to the enhancement of photocatalytic activity of P25. Three types of sodium salts (NaCl, $NaNO_3$, and Na_2SO_4) were used to replace Na_2CO_3 to evaluate the possible effects of Na^+ on the photocatalytic activity of the modified P25. As seen in Table 1, the PCO of SO_2 was not improved with these modified catalysts. In contrast, the photo-reaction breakthrough time (t_{rb}) of P25 decreased from 28 min to 20, 15, and 20 min for the P25 modified by NaCl, $NaNO_3$, and Na_2SO_4, respectively. The inhibition of the photocatalytic reaction could probably be caused by several reasons as follows. The adsorption ability of P25 decreased after washing with the aforementioned sodium salts. This change of performance was mainly caused by the occupation of SO_2 adsorption sites on the surface of the catalyst. Besides, the coverage of the sodium salts on the catalyst surface prevented the UV irradiation from reaching the TiO_2, and consequently lowered the photocatalytic oxidation reaction.

The third column, pH, in Table 1, were recorded when Na_2CO_3 solution was used to modify P25. There are abundant hydroxyl groups (OH^-) in the 0.2M Na_2CO_3 aqueous solution with pH11.8. The hydroxyl groups were likely bounded to the catalyst surface and they improved the photocatalytic activity of P25. This hypothesis was tested by examining the performance of the catalyst modified with 0.01M NaOH (pH=12) instead of 0.2M Na_2CO_3 (pH=11.8). Comparison between the results of P25-0.2M-Na_2CO_3 and P25-0.01M-NaOH in Table 1 shows that the PCO activity of P25 modified by NaOH was much lower than that by Na_2CO_3 despite of the higher OH^- concentration in NaOH. The result confirms that the hydroxyl groups in Na_2CO_3 solution were not the main factor that contributed to the enhancement in the photocatalytic activity of P25.

In summary, the enhanced photocatalytic activity of P25 for PCO of SO_2 was attributed to the carbonate/bicarbonate ions deposited on the surface of catalyst.

Figure 6 and Table 1 show that the catalyst activity increased dramatically with increasing the Na_2CO_3 from 0.005M to 0.2M. The corresponding mechanisms were investigated and analyzed by characterizing the modified catalysts in the following sections.

3.3. On the mechanisms of enhanced PCO activity of P25

3.3.1. XRD and UV-Vis results

Figure S2 shows crystalline phases of P25 before and after catalyst modification. The diffraction peaks of the modified catalysts were in consistent with those of pure P25, which showed both anatase and rutile phases [44]. There are no observable changes in the peak positions, numbers, and intensities of the XRD patterns among the modified samples. This indicates the modification did not affect the crystallographic structure of P25.

Figure S3 shows the UV-Vis absorbance spectra of P25 modified with different chemicals. The same absorption edge for different catalysts indicates that the accumulation of the carbonate salts on the catalyst surface did not affect the band gap of the P25 catalyst composites. This also indicates that the enhancement of the photocatalytic activity by Na_2CO_3 was not caused by the change of irradiation absorption. However, the absorbance of UV irradiation with the wavelength less than 350 nm decreased slightly because of the deposition of Na_2CO_3 on the catalyst surface, which affects the photo-activity adversely. As Figure 5 shows, the photocatalytic activity of TiO_2 increased remarkably with increasing Na_2CO_3 concentration from 0.005M to 0.2M. This indicates that the improvement in the PCO ability caused by CO_3^{2-} outweighed the aforementioned adverse effects. Nevertheless, further increasing the concentration of Na_2CO_3 will cause more surface coverage of TiO_2. At certain point, UV irradiation will be blocked and could not reach the TiO_2 surface, and the catalyst lost its photocatalytic activity (see blank test results in Figure 4). The adverse effects of

the surface coverage dominated the whole process in this scenario. In a word, there must be an optimum modification concentration of Na_2CO_3 for the photocatalytic activity of TiO_2, which needs to be determined in the further study.

3.3.2. Formation of oxidative species on the modified P25 surface

The catalyst modification with Na_2CO_3 resulted in the deposition of CO_3^{2-} on the TiO_2 surface. The redox-couple $CO_3^{\bullet-}$/ CO_3^{2-} has a potential of 1.59V (vs. NHE) [45], which is more negative than the valence band of TiO_2 as shown in Figure 7. From a thermodynamics point of view, the redox-couples on the catalyst surface can be oxidized by the valence band holes if their redox potential is more negative than the energy level of the top of valence band [46]. As a result, the oxidation of CO_3^{2-} to $CO_3^{\bullet-}$ by the photo-generated holes could take place through the following two reactions

$$CO_3^{2-} + h^+ \rightarrow CO_3^{\bullet-} \quad (6)$$

$$HCO_3^- + h^+ \rightarrow CO_3^{\bullet-} + H^+ \quad (7)$$

In addition, due to the lower redox potential of $CO_3^{\bullet-}$/ CO_3^{2-} than that of the $\bullet OH/OH^-$ (1.9 V) or $\bullet OH/H_2O$ (2.73 V) [47], a large amount of •OH radicals in Na_2CO_3 [18] and $NaHCO_3$ [48] solutions were consumed by CO_3^{2-} and HCO_3^- through the following equations:

$$CO_3^{2-} + \bullet OH \rightarrow CO_3^{\bullet-} + OH^- \quad (8)$$

$$HCO_3^- + \bullet OH \rightarrow CO_3^{\bullet-} + H_2O \quad (9)$$

The increase of the PCO ability of P25 upon the addition of Na_2CO_3 indicates an increase in the formation of oxidative species.

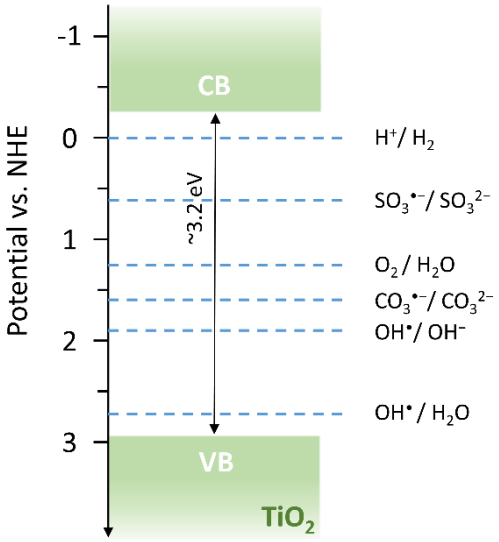

Figure 7 TiO_2 band gap and redox potentials (vs. NHE) for different redox-couples (based on the data in ref.[4, 45, 47, 49])

This hypothesis is confirmed with the low temperature ESR (113K) and spin-trapping analysis, which examined the role of carbonate in the generation of oxidative species on illuminated P25 surface. Figure 8 shows the ESR spectra recorded at 113K for catalysts under UV irradiation. The signals of P25 corresponding to g-values of g_x=2.003, g_y=2.014, and g_z=2.026 can be assigned to the TiO_2 surface oxygen-related radicals ($Ti^{4+}O^{\bullet-}$) [50, 51]. They are resulted from the trapping of holes on the illuminated catalyst surface.

The intensity of the spectrum was dramatically enhanced after the modification of Na_2CO_3. The results of UV-Vis analysis indicate that the modification of Na_2CO_3 did not change the band gap or the UV absorbance intensity of TiO_2 (shown in Figure S3). Thus the ability of TiO_2 under the same UV irradiation to generate electron-hole pairs is believed to be similar before and after the modification. However, the intensity of the ESR spectrum increased greatly after the modification. This indicates more electron-hole pairs were able to separate from each other and move toward the catalyst surface to be captured. The ESR spectrum intensity became stronger with a higher concentration of modification reagent. This is in line with the observations in Figure 6, which shows that the photocatalytic activity increased with increasing the Na_2CO_3

concentration.

The new ESR signal of $CO_3^{\bullet-}$ was observed for P25 samples modified with Na_2CO_3. Those corresponding to the g values of g_x =2.007, g_y =2.010, and g_z =2.018 are in agreement with literature for $CO_3^{\bullet-}$ on the γ-irradiated $KHCO_3$ surface [52] and the UV-irradiated Na_2CO_3/TiO_2 mixture [51].

The ESR spectra were simulated using the BiomolecularEPRSpectroscopy software developed by Hagen [53]. The simulated spectra are shown in dash lines in Figure 8. The spectrum of $CO_3^{\bullet-}$ overlapped with the holes trapping spectrum of $Ti^{4+}O^{\bullet-}$. According to the simulation results, the contributions of $CO_3^{\bullet-}$ signal to the total intensity were 60% and 67% for 0.1 and 0.2 M Na_2CO_3 modified samples, respectively. Therefore, the enhancement of the ESR spectrum after modification was mainly due to the formation of $CO_3^{\bullet-}$. Consequently, after Na_2CO_3 modification, the carbonate and bicarbonate ions accumulated on P25 surface acted as electron donors and trap photo-generated holes on the valance band. The trapping of holes suppressed the electron-hole recombination and increased the photocatalytic activity as indicated by the ESR spectra in Figure 8.

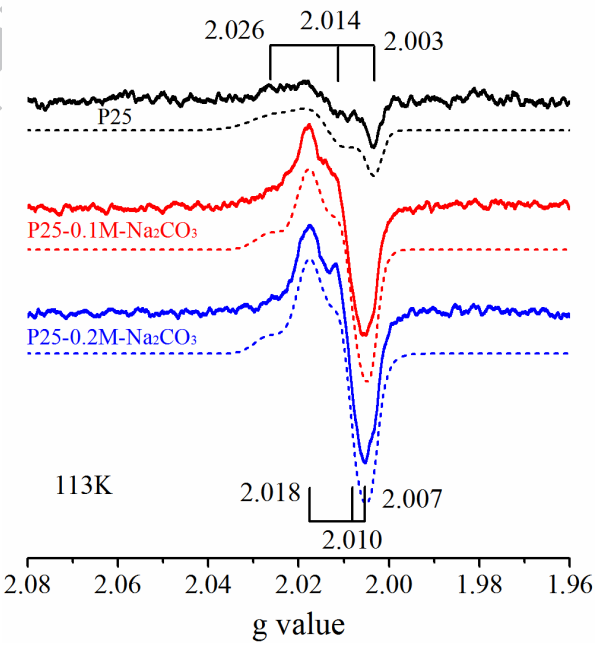

Figure 8. ESR spectra of P25 catalysts modified with Na_2CO_3 (Dash lines: simulation spectra. Solid lines: experimental results)

Figure 9 shows the ESR spin trapping spectra of different TiO_2 suspensions with various concentrations of Na_2CO_3. Negligible spin-adducts were formed under dark condition, whereas the formation of spin-adduct [DMPO-OH] ($a_N=a_H^{\beta}$=1.49mT and g=2.006) was observed under UV irradiation (Figure 9 (b)). The [DMPO-OH] intensity increased with increasing Na_2CO_3 concentration, suggesting that the production of •OH radicals on the TiO_2 surface was possibly promoted by Na_2CO_3. As shown in Eqs. (1) to (4), the •OH radicals are important oxidants in the PCO of SO_2. This also explains why the photocatalytic reaction time was prolonged by increasing Na_2CO_3 concentration (Figure 6 and Table 1). All this leads to a conclusion that the increment of •OH may be one of the most important reasons behind the improvement in the photocatalytic oxidation of SO_2.

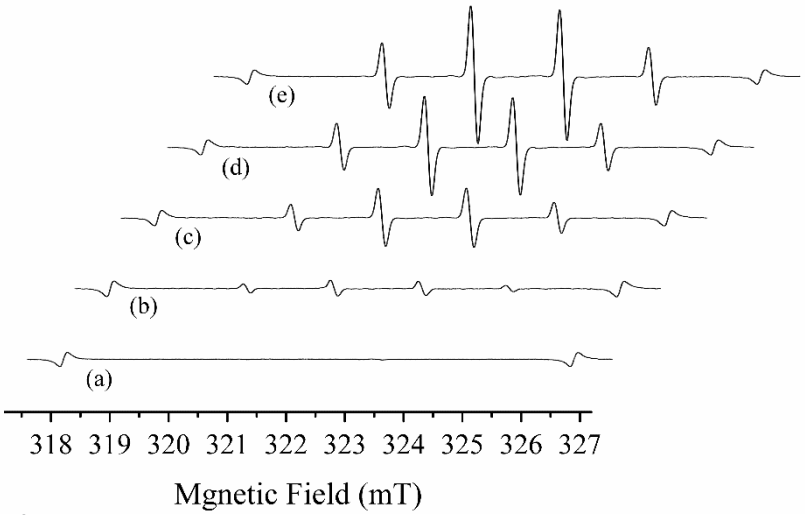

Figure 9. ESR spectra of TiO_2 suspensions at room temperature with 50mM DMPO in different solutions ((a) in H_2O under dark condition, and in (b) H_2O, (c) 0.05M, (d) 0.1M, and (e) 0.2M aqueous Na_2CO_3 under UV irradiation for 1 min).

However, the mechanisms behind the increase of [DMPO-OH] adducts in the presence of carbonate is not clear. The formation of •OH radicals on the irradiated TiO_2 surface has been investigated both experimentally and theoretically by other researchers [54]. Two main pathways were proposed and shown in Figure 10 [4, 54]: one is through the reaction between surface bounded H_2O/OH^- and valence band

holes (Figure 10 (a)), and the other is through the photo-reduction of adsorbed O_2 by the conduction band electrons (Figure 10 (b)).

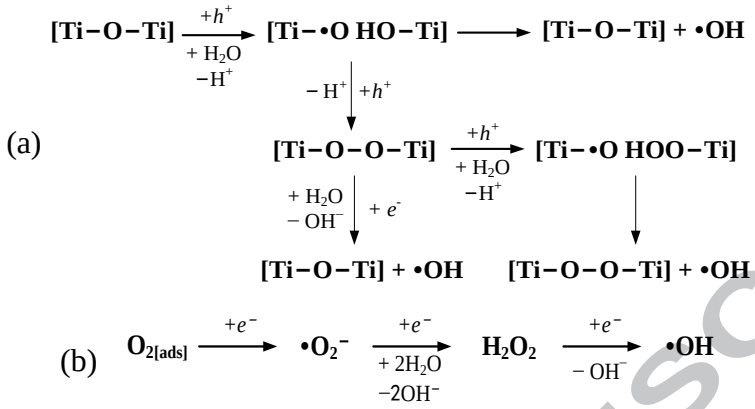

Figure 10. Photocatalytic pathways for the generation of hydroxyl radicals ((a) through valence band holes, (b) through conduction band electrons).

It is proposed in this study that the addition of Na_2CO_3 suppressed the electron-hole recombination and caused the increase of •OH most likely through Figure 10 (b), which increased the [DMPO-OH] intensity. The low temperature ESR spectra (see Figure 8) indicated the trapping of the valence band holes by carbonate and bicarbonate ions. The role of carbonate ions as the hole scavenger to form $CO_3^{\bullet-}$ was also reported by others for aqueous solutions [17]. If Figure 10 (a) had dominated the production pathway of •OH, the competitive effects would have decreased the concentration of •OH radicals, but this was not supported by the results in the present study. In contrast, the intensity of •OH trapping adducts gradually increased with the addition of Na_2CO_3 as shown in Figure 9. Similar results were reported by other researchers using $NaHCO_3$ [55]. The trapping of valance band holes by carbonate and bicarbonate increased the lifetime of photoinduced electrons by hindering the electron-hole recombination, which could increase the amount of •OH radicals through the pathway (b) in Figure 10.

On the other hand, it was reported that $CO_3^{\bullet-}$ can be trapped by DMPO and eventually

form [DMPO-OH] adducts [56, 57], which may affect the detection of the original •OH radicals. The $CO_3^{\bullet-}$ can be formed through the capture of valence band holes (Reactions 6 and 7) or the consumption of •OH (Reactions 8 and 9). The increase in [DMPO-OH] intensity with increasing Na_2CO_3 concentration could be caused by the reaction between DMPO and $CO_3^{\bullet-}$ instead of the increasing of •OH itself. However, DMPO is more competitive than CO_3^{2-}/ HCO_3^- in reacting with •OH. The rate constant of DMPO trapping with •OH, which is 4.3×10^9 $M^{-1}s^{-1}$[57], is about 10-fold and 1000-fold greater than those for Reactions (8) (3×10^8 $M^{-1}s^{-1}$) and (9) (8.5×10^6 $M^{-1}s^{-1}$)[58], respectively. As such, the existing •OH would prefer to react with DMPO instead of consuming by CO_3^{2-}/ HCO_3^-. In addition, the improved performance of P25 would mainly be attributed to $CO_3^{\bullet-}$ radicals if $CO_3^{\bullet-}$ dominates the increase of [DMPO-OH] instead of •OH on the irradiated P25-Na_2CO_3 surface. As seen below, additional experiments with P25-0.2M-Na_2CO_3 in the absence of O_2 and H_2O showed that the $CO_3^{\bullet-}$ alone could not react effectively with SO_2.

Figure 11 shows the effects of O_2 and H_2O on the photocatalytic activity of P25-0.2M-Na_2CO_3. SO_2 cannot be effectively oxidized without O_2 and H_2O in the flue gas, although Na_2CO_3 can enhance the hole trapping ability of the catalyst by forming $CO_3^{\bullet-}$ (as explained above in Figure 8). Addition of 5 vol% O_2 into the flue gas led to a slight decrease in SO_2 penetration rate. With 2.9 vol% H_2O in the gas flow, the SO_2 concentration at the outlet decreased to zero and maintained this status for about 300 min. This is close to the t_{rb} (297 min) of P25-0.2M-Na_2CO_3 (see Figure 5), where H_2O and O_2 were added from the beginning. In other words, the enhancement of the photocatalytic activity of P25 by Na_2CO_3 can only be achieved with the presence of H_2O.

Even though $CO_3^{\bullet-}$ and $O_2^{\bullet-}$ can be formed without H_2O, the reaction rate was much lower than that in the presence of H_2O. Regardless of the pathway in Figure 10, H_2O

is always needed for the formation of •OH. Carbonate radicals ($CO_3^{\bullet-}$) was reported to be much less reactive than •OH when reacting with sulfite; the rate constants for $CO_3^{\bullet-}$ (Eq. (10)) and •OH ((Eq. (11))) are 1×10^7 and 5.5×10^9 M^{-1} s^{-1}, respectively [49]. The formed $SO_3^{\bullet-}$ can further produce SO_3 through Eq. (12). The rate constant for the reaction between $O_2^{\bullet-}$ and sulfite was reported only 82 $M^{-1}s^{-1}$, which is much smaller that of $CO_3^{\bullet-}$ and •OH [59]. Since •OH plays a more important role than $CO_3^{\bullet-}$ in the PCO of SO_2, the reaction rate of SO_2 would decrease if •OH was consumed by CO_3^{2-}/HCO_3^-. Nevertheless, the addition of Na_2CO_3 improved the PCO of SO_2 as shown in Figure 5. Therefore, the consumption of •OH by CO_3^{2-}/HCO_3^- should have a minor impact on the formation of •OH for the experimental conditions within this study. It is worth noting that the reaction rate between •OH and sulfite is about 10 times faster than that between •OH and CO_3^{2-}, and 1000 times faster than that between •OH and HCO_3^-. Consequently, most •OH would react with the adsorbed SO_2 rapidly instead of consuming by CO_3^{2-}/HCO_3^-.

$$SO_3^{2-} + CO_3^{\bullet-} \rightarrow SO_3^{\bullet-} + CO_3^{2-} \quad (10)$$

$$SO_3^{2-} + \bullet OH \rightarrow SO_3^{\bullet-} + OH^- \quad (11)$$

$$2SO_3^{\bullet-} \rightarrow SO_3 + SO_3^{2-} \quad (12)$$

In summary, the addition of H_2O caused the production of •OH on the irradiated P25 surface and this process could be promoted by the presence of Na_2CO_3 through the scheme described in Figure 10 (b). As a result, the PCO performance of P25 improved.

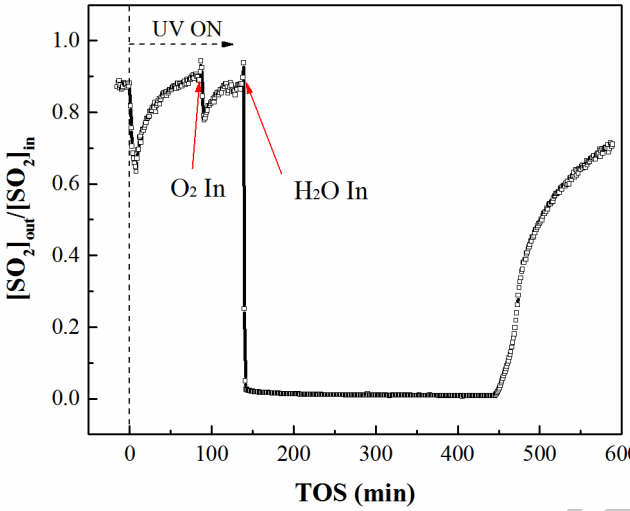

Figure 11. Effects of O_2 and H_2O on the photocatalytic oxidation of SO_2 using P25-0.2M-Na_2CO_3

3.3.3. The roles of CO_3^{2-} and HCO_3^-

When P25 was modified using Na_2CO_3 solution, both carbonate and bicarbonate ions exist in solution and could deposit on catalyst surface. The concentration distribution of CO_3^{2-} and HCO_3^- can be determined by using the proton balance equations (PBE) for the ionization of Na_2CO_3 in solutions:

$$[CO_3^{2-}] = \frac{[C_t][OH^-]^2}{k_{b1} \bullet k_{b2} + k_{b1}[OH^-] + [OH^-]^2} \quad (13)$$

$$[HCO_3^-] = \frac{k_{b1}[C_t][OH^-]}{k_{b1} \bullet k_{b2} + k_{b1}[OH^-] + [OH^-]^2} \quad (14)$$

where k_{b1}=1.79×10^{-4} and k_{b2}=2.33×10^{-8} are the primary and secondary hydrolysis constants, respectively; $[C_t]$ is the total carbon concentration which equals to the Na_2CO_3 concentration; $[OH^-]$ is the concentration of hydroxyl ions in Na_2CO_3 solution.

Figure 12 shows the distributions of CO_3^{2-} and HCO_3^- in different concentrations of Na_2CO_3 solution. They were calculated using Eqs. (13) and (14). As $[Na_2CO_3]$ decreased, the share of CO_3^{2-} in the total carbon species decreased while that of

HCO_3^- increased gradually. When [Na_2CO_3] decreased to 0.05M or lower, the share of CO_3^{2-} began to decrease sharply, and more carbon species are presented in the form of HCO_3^-. Consequently, for a solution with low concentration of Na_2CO_3, considerable amount of carbon in the solution would present as HCO_3^- and deposited on catalyst surface after the catalyst modification process.

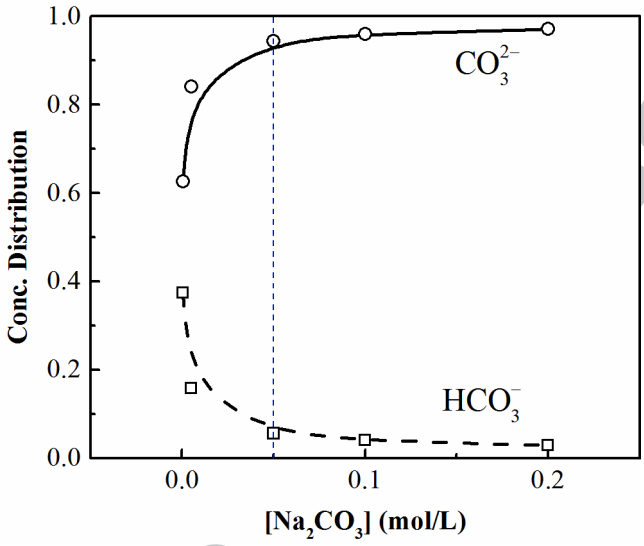

Figure 12. Distribution of CO_3^{2-} and HCO_3^- versus the Na_2CO_3 concentration

As shown in Figure 5 and Figure 6, the enhancement in the activity of P25 was closely related to the concentration of Na_2CO_3. With a Na_2CO_3 concentration lower than 0.05M, the enhancement of the photocatalytic activity was much smaller than the one modified with 0.2M Na_2CO_3. The adsorption ability of the latter was about 2.3 times greater than the former, while the photo-reaction with SO_2 was 6.4 times greater. Similar results were reported by Sayama et.al. [19] when Na_2CO_3 was added to liquid water to improve the water-splitting process with Pt doped TiO_2 as catalyst. They found that only concentrated Na_2CO_3 solutions was able to dramatically boost the H_2 and O_2 splitting rates. In this study P25 modified with 0.2M $NaHCO_3$ showed four times less photocatalytic activity than that with P25-0.2M-Na_2CO_3 (see Table 1). This indicates that the accumulated $NaHCO_3$ on catalyst surface had a much less impact on the catalyst activity than Na_2CO_3 did. Although both HCO_3^- and CO_3^{2-} can act as

electron donors to produce $CO_3^{\bullet-}$ and promote the production of •OH as discussed above, the reactivity of HCO_3^- is much less than that of CO_3^{2-}[58]. Figure 13 shows the ESR spectra of spin trap for TiO_2 suspensions in Na_2CO_3 and $NaHCO_3$ solutions. Even with the same anion concentration, the intensity of [DMPO-OH] in Na_2CO_3 was much stronger than that in $NaHCO_3$ solutions. This is consistent with the experimental results presented in Table 1. The lower efficiency in the PCO of SO_2 was mainly caused by the lower reactivity of HCO_3^- compared with CO_3^{2-}.

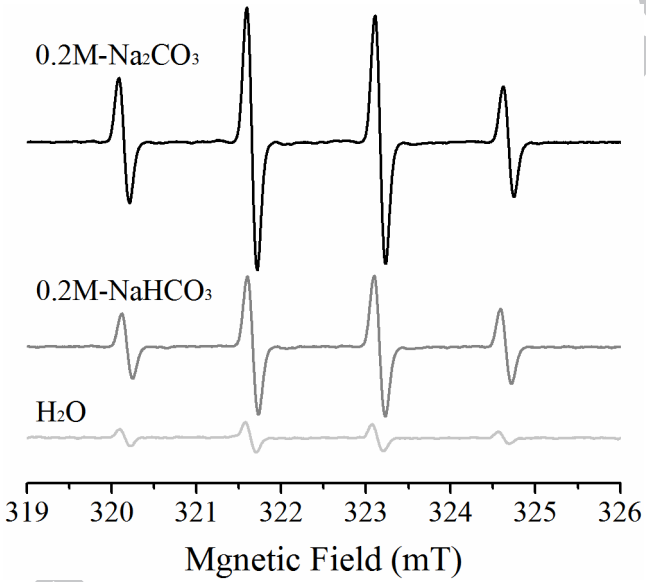

Figure 13. ESR spectra of TiO_2 suspensions at room temperature in different solutions under UV illumination for 1 min.

3.4. Recycle stability for the Na_2CO_3 modified P25

As seen in Figure 5 and Table 1, even though the modification can prolong the photoreaction breakthrough time and improve the SO_2 conversion capacity of TiO_2, the modified catalyst still suffers from the deactivation caused by the adsorption of the PCO products on its surface. To test the stability of catalyst recycling and the regeneration, the used (deactivated) P25-0.2M-Na_2CO_3 was regenerated with the same solution following the same procedure described in section 2.1.

Figure 14 shows the SO_2 capacity and the reaction breakthrough time t_{rb} for the

modified TiO_2 with different recycle times. It can be seen that after fifth recycle, the activity of the catalyst could still be improved for SO_2 treatment comparing with that of P25 only. Furthermore, the capacity and the breakthrough time are close to the first recycle. However, fluctuation exists for different recycle times, which is most likely caused by the slight difference in the modification procedure during the experiments. In general, the reactivity of the modified catalyst is stable with the average capacity and t_{rb} being 62.5 mg SO_2/g TiO_2 and 309 min, respectively. The activity of the deactivated catalyst can be recovered by washing and drying.

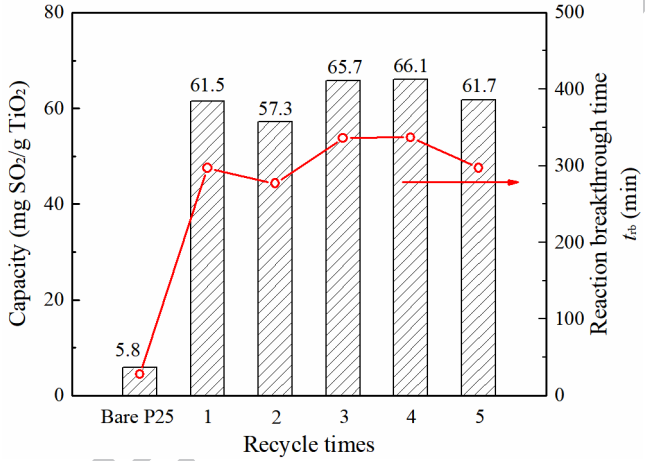

Figure 14. Capacity and reaction breakthrough time of P25-0.2M-Na_2CO_3 vs. recycle time.

4. Conclusions

In this study, the photocatalytic abilities of TiO_2 (P25) modified with Na_2CO_3 of different concentrations were investigated. The PCO of SO_2 with P25 was enhanced by 1.04, 1.64, 4.96 and 10.6 times when P25 was modified with 0.005, 0.05, 0.1 and 0.2M Na_2CO_3, respectively. The enhancement was caused by 1) the improvement in the adsorption ability of P25 due to the reaction between Na_2CO_3 and SO_2, and 2) the positive effects of Na_2CO_3 on the photocatalytic activity of TiO_2 under UV-irradiation. The enhancement of the photocatalytic activity of P25 by Na_2CO_3 was only observed in the presence of H_2O, which emphasizes the important role of H_2O in the PCO of SO_2. Low temperature (113K) ESR reveals that Na_2CO_3 boosted the separation of

electron-hole pairs by trapping valance band holes to form carbonate radicals ($CO_3^{\bullet-}$). In addition, the intensity of [DMPO-OH] adducts increased with increasing Na_2CO_3 concentration because more reactive species were formed on P25 surface. Na_2CO_3 deposited on the catalyst surface could inhibit the recombination of electron-hole and promote the generation of hydroxyl radicals (•OH) most likely through the photo-reduction of adsorbed O_2 by the conduction band electrons. The promoted generation of •OH reacted with SO_2 rapidly and improved the PCO ability of P25. As the concentration of Na_2CO_3 decreased to less than 0.05M, more carbonate ions presented in the form of HCO_3^- and deposited on P25 surface. However, HCO_3^- was found to be less active than CO_3^{2-} on P25 surface, which caused the improvement of P25 to be minor when modifying at a low Na_2CO_3 concentration (<0.05M).

Acknowledgement

The authors would like to thank Joerg Ahne for proof reading the manuscript. Financial support was provided by National Key Research and Development Program of China (2017YFB0603903) and Tsinghua University – University of Waterloo Joint Research Centre for Micro/Nano Energy & Environment Technologies operating grant.

References

[1] A. Di Paola, E. Garcia-Lopez, G. Marci, L. Palmisano, A survey of photocatalytic materials for environmental remediation, J. Hazard. Mater. 211-212 (2012) 3-29.

[2] W. Cui, J. Li, F. Dong, Y. Sun, G. Jiang, W. Cen, S.C. Lee, Z. Wulle, Highly Efficient Performance and Conversion Pathway of Photocatalytic NO Oxidation on SrO-Clusters@Amorphous Carbon Nitride, Environ. Sci. Technol. 51 (2017) 10682-10690.

[3] X. Dong, J. Li, Q. Xing, Y. Zhou, H. Huang, F. Dong, The activation of reactants and intermediates promotes the selective photocatalytic NO conversion on electron-localized Sr-intercalated g-C_3N_4, Appl. Catal. B 232 (2018) 69-76.

[4] A. Fujishima, X.T. Zhang, D.A. Tryk, TiO_2 photocatalysis and related surface

phenomena, Surf. Sci. Rep. 63 (2008) 515-582.

[5] D. Zhao, G. Sheng, C. Chen, X. Wang, Enhanced photocatalytic degradation of methylene blue under visible irradiation on graphene@TiO_2 dyade structure, Appl. Catal. B 111-112 (2012) 303-308.

[6] J. Schneider, M. Matsuoka, M. Takeuchi, J. Zhang, Y. Horiuchi, M. Anpo, D.W. Bahnemann, Understanding TiO_2 photocatalysis: mechanisms and materials, Chem. Rev. 114 (2014) 9919-9986.

[7] S.G. Kumar, L.G. Devi, Review on modified TiO_2 photocatalysis under UV/visible light: selected results and related mechanisms on interfacial charge carrier transfer dynamics, J. Phys. Chem. A 115 (2011) 13211-13241.

[8] H. Park, Y. Park, W. Kim, W. Choi, Surface modification of TiO_2 photocatalyst for environmental applications, J. Photochem. Photobiol. C: Photochem. Rev. 15 (2013) 1-20.

[9] A. Naldoni, M. D'Arienzo, M. Altomare, M. Marelli, R. Scotti, F. Morazzoni, E. Selli, V. Dal Santo, Pt and Au/TiO_2 photocatalysts for methanol reforming: Role of metal nanoparticles in tuning charge trapping properties and photoefficiency, Appl. Catal. B 130-131 (2013) 239-248.

[10] J. Long, H. Chang, Q. Gu, J. Xu, L. Fan, S. Wang, Y. Zhou, W. Wei, L. Huang, X. Wang, Gold-plasmon enhanced solar-to-hydrogen conversion on the {001} facets of anatase TiO_2 nanosheets, Energy Environ. Sci. 7 (2014) 973-977.

[11] J. Shi, J. Chen, G. Li, T. An, H. Yamashita, Fabrication of Au/TiO_2 nanowires@carbon fiber paper ternary composite for visible-light photocatalytic degradation of gaseous styrene, Catal. Today 281 (2017) 621-629.

[12] Y. Cong, X.K. Li, Y. Qin, Z.J. Dong, G.M. Yuan, Z.W. Cui, X.J. Lai, Carbon-doped TiO_2 coating on multiwalled carbon nanotubes with higher visible light photocatalytic activity, Appl. Catal. B 107 (2011) 128-134.

[13] K.F. Zhou, Y.H. Zhu, X.L. Yang, X. Jiang, C.Z. Li, Preparation of graphene-TiO_2 composites with enhanced photocatalytic activity, New J. Chem. 35 (2011) 353-359.

[14] H. Sheng, Q. Li, W. Ma, H. Ji, C. Chen, J. Zhao, Photocatalytic degradation of organic pollutants on surface anionized TiO_2: Common effect of anions for high hole-availability by water, Appl. Catal. B 138-139 (2013) 212-218.

[15] J. Yu, W. Wang, B. Cheng, B.-L. Su, Enhancement of photocatalytic activity of mesporous TiO_2 powders by hydrothermal surface fluorination treatment, J. Phys. Chem. C 113 (2009) 6743-6750.

[16] M.C. Hidalgo, M. Maicu, J.A. Navío, G. Colón, Study of the synergic effect of sulphate pre-treatment and platinisation on the highly improved photocatalytic activity of TiO_2, Appl. Catal. B 81 (2008) 49-55.

[17] X. Xiong, X. Zhang, Y. Xu, Incorporative Effect of Pt and Na_2CO_3 on TiO_2-Photocatalyzed Degradation of Phenol in Water, J. Phys. Chem. C 120 (2016) 25689-25696.

[18] A. Kumar, N. Mathur, Photocatalytic degradation of aniline at the interface of

TiO_2 suspensions containing carbonate ions, J. Colloid Interface Sci. 300 (2006) 244-252.

[19] K. Sayama, H. Arakawa, Effect of carbonate salt addition on the photocatalytic decomposition of liquid water over Pt–TiO_2 catalyst, J. Chem. Soc., Faraday Trans. 93 (1997) 1647-1654.

[20] H. Arakawa, K. Sayama, Solar hydrogen production. Significant effect of Na_2CO_3 addition on water splitting using simple oxide semiconductor photocatalysts, Catal. Surv. JPN. 4 (2000) 75-80.

[21] H. Chen, O. Zahraa, M. Bouchy, Inhibition of the adsorption and photocatalytic degradation of an organic contaminant in an aqueous suspension of TiO_2 by inorganic ions, J. Photochem. Photobiol. A: Chem. 108 (1997) 37-44.

[22] B. Gao, P.S. Yap, T.M. Lim, T.-T. Lim, Adsorption-photocatalytic degradation of Acid Red 88 by supported TiO_2: Effect of activated carbon support and aqueous anions, Chem. Eng. J. 171 (2011) 1098-1107.

[23] N. Bouanimba, N. Laid, R. Zouaghi, T. Sehili, Effect of pH and inorganic salts on the photocatalytic decolorization of methyl orange in the presence of TiO_2 P25 and PC500, Desalination Water Treat. 53 (2015) 951-963.

[24] C.F. You, X.C. Xu, Coal combustion and its pollution control in China, Energy 35 (2010) 4467-4472.

[25] H.H. Chen, C.E. Nanayakkara, V.H. Grassian, Titanium Dioxide Photocatalysis in Atmospheric Chemistry, Chem. Rev. 112 (2012) 5919-5948.

[26] Y. Dupart, S.M. King, B. Nekat, A. Nowak, A. Wiedensohler, H. Herrmann, G. David, B. Thomas, A. Miffre, P. Rairoux, Mineral dust photochemistry induces nucleation events in the presence of SO_2, PNAS 109 (2012) 20842-20847.

[27] C.E. Nanayakkara, W.A. Larish, V.H. Grassian, Titanium Dioxide Nanoparticle Surface Reactivity with Atmospheric Gases, CO_2, SO_2, and NO_2: Roles of Surface Hydroxyl Groups and Adsorbed Water in the Formation and Stability of Adsorbed Products, J. Phys. Chem. C 118 (2014) 23011-23021.

[28] C.H. Ao, S.C. Lee, Combination effect of activated carbon with TiO_2 for the photodegradation of binary pollutants at typical indoor air level, J. Photochem. Photobiol., A 161 (2004) 131-140.

[29] C.H. Ao, S.C. Lee, S.C. Zou, C.L. Mak, Inhibition effect of SO_2 on NOx and VOCs during the photodegradation of synchronous indoor air pollutants at parts per billion (ppb) level by TiO_2, Appl. Catal. B 49 (2004) 187-193.

[30] C.Y. Su, X. Ran, J.L. Hu, C.L. Shao, Photocatalytic Process of Simultaneous Desulfurization and Denitrification of Flue Gas by TiO_2-Polyacrylonitrile Nanofibers, Environ. Sci. Technol. 47 (2013) 11562-11568.

[31] J. Bao, Y. Dai, H. Liu, L. Yang, Photocatalytic removal of SO_2 over Mn doped titanium dioxide supported by multi-walled carbon nanotubes, Int. J. Hydrogen Energy 41 (2016) 15688-15695.

[32] Y. Han, J. Zhang, Y. Zhao, Visible-light-induced photocatalytic oxidation of nitric oxide and sulfur dioxide: Discrete kinetics and mechanism, Energy 103 (2016)

725-734.

[33] H. Wang, D. Xie, Q. Chen, C. You, Kinetic modeling for the deactivation of TiO_2 during the photocatalytic removal of low concentration SO_2, Chem. Eng. J. 303 (2016) 425-432.

[34] H. Wang, C. You, Photocatalytic removal of low concentration SO_2 by titanium dioxide, Chem. Eng. J. 292 (2016) 199-206.

[35] L. Wang, Y. Zhao, J. Zhang, Photochemical Removal of SO_2 over TiO_2-Based Nanofibers by a Dry Photocatalytic Oxidation Process, Energy Fuels 31 (2017) 9905-9914.

[36] G. Rubasinghege, S. Elzey, J. Baltrusaitis, P.M. Jayaweera, V.H. Grassian, Reactions on Atmospheric Dust Particles: Surface Photochemistry and Size-Dependent Nanoscale Redox Chemistry, J. Phys. Chem. Lett. 1 (2010) 1729-1737.

[37] H. Liu, X.Q. Yu, H.M. Yang, The integrated photocatalytic removal of SO_2 and NO using Cu doped titanium dioxide supported by multi-walled carbon nanotubes, Chem. Eng. J. 243 (2014) 465-472.

[38] J. Baltrusaitis, P.M. Jayaweera, V.H. Grassian, Sulfur Dioxide Adsorption on TiO_2 Nanoparticles: Influence of Particle Size, Coadsorbates, Sample Pretreatment, and Light on Surface Speciation and Surface Coverage, J. Phys. Chem. C 115 (2011) 492-500.

[39] A. Yamamoto, K. Teramura, S. Hosokawa, T. Tanaka, Effects of SO_2 on selective catalytic reduction of NO with NH_3 over a TiO_2 photocatalyst, Sci. Technol. Adv. Mater. 16 (2015) 1-9.

[40] R. Jaworowski, S. Mack, Evaluation of Methods for Measurement of SO_3/H_2SO_4 in Flue Gas, J. Air Pollut. Control Assoc. 29 (1979) 43-46.

[41] U. Tumuluri, J.D. Howe, W.P. Mounfield, M. Li, M. Chi, Z.D. Hood, K.S. Walton, D.S. Sholl, S. Dai, Z. Wu, Effect of Surface Structure of TiO_2 Nanoparticles on CO_2 Adsorption and SO_2 Resistance, ACS Sustain. Chem. Eng. 5 (2017) 9295-9306.

[42] J. Baltrusaitis, J. Schuttlefield, E. Zeitler, V.H. Grassian, Carbon dioxide adsorption on oxide nanoparticle surfaces, Chem. Eng. J. 170 (2011) 471-481.

[43] A. Shchukarev, D. Korolkov, XPS study of group IA carbonates, Open Chemistry 2 (2004) 347-362.

[44] Z. Jin, W.B. Duan, B. Liu, X.D. Chen, F.H. Yang, J.P. Guo, Fabrication of efficient visible light activated Cu-P25-graphene ternary composite for photocatalytic degradation of methyl blue, Appl. Surf. Sci. 356 (2015) 707-718.

[45] R.E. Huie, C.L. Clifton, P. Neta, Electron transfer reaction rates and equilibria of the carbonate and sulfate radical anions, Int. J. Rad. Appl. Instrum. C 38 (1991) 477-481.

[46] O. Carp, C.L. Huisman, A. Reller, Photoinduced reactivity of titanium dioxide, Prog. Solid State Chem. 32 (2004) 33-177.

[47] H. Kornweitz, D. Meyerstein, The plausible role of carbonate in photo-catalytic

water oxidation processes, Phys. Chem. Chem. Phys. 18 (2016) 11069-11072.
[48] T. Eriksen, J. Lind, G. Merenyi, On the acid-base equilibrium of the carbonate radical, Radiat. Phys. Chem. 26 (1985) 197-199.
[49] P. Neta, R.E. Huie, Free-radical chemistry of sulfite, Environ. Health Perspect. 64 (1985) 209.
[50] C.P. Kumar, N.O. Gopal, T.C. Wang, M.-S. Wong, S.C. Ke, EPR investigation of TiO_2 nanoparticles with temperature-dependent properties, J. Phys. Chem. B 110 (2006) 5223-5229.
[51] N.M. Dimitrijevic, B.K. Vijayan, O.G. Poluektov, T. Rajh, K.A. Gray, H. He, P. Zapol, Role of water and carbonates in photocatalytic transformation of CO_2 to CH4 on titania, J. Am. Chem. Soc. 133 (2011) 3964-3971.
[52] R. Serway, S. Marshall, Electron Spin Resonance Absorption Spectra of CO_3^- and CO_3^{3-} Molecule—Ions in Irradiated Single- Crystal Calcite, J. Chem. Phys. 46 (1967) 1949-1952.
[53] W.R. Hagen, Biomolecular EPR spectroscopy, CRC press2008.
[54] Y. Nosaka, A.Y. Nosaka, Generation and Detection of Reactive Oxygen Species in Photocatalysis, Chem. Rev. 117 (2017) 11302-11336.
[55] A. Molinari, L. Samiolo, R. Amadelli, EPR spin trapping evidence of radical intermediates in the photo-reduction of bicarbonate/CO_2 in TiO_2 aqueous suspensions, Photochem Photobiol Sci 14 (2015) 1039-1046.
[56] H. Zhang, J. Joseph, M. Gurney, D. Becker, B. Kalyanaraman, Bicarbonate enhances peroxidase activity of cu, zn-superoxide dismutase role of carbonate anion radical and scavenging of carbonate anion radical by metalloporphyrin antioxidant enzyme mimetics, J. Biol. Chem. 277 (2002) 1013-1020.
[57] C. Karunakaran, H. Zhang, J. Joseph, W.E. Antholine, B. Kalyanaraman, Thiol oxidase activity of copper, zinc superoxide dismutase stimulates bicarbonate-dependent peroxidase activity via formation of a carbonate radical, Chem. Res. Toxicol. 18 (2005) 494-500.
[58] O. Augusto, M.G. Bonini, A.M. Amanso, E. Linares, C.C. Santos, S.l.L. De Menezes, Nitrogen dioxide and carbonate radical anion: two emerging radicals in biology, Free Radical Biol. Med. 32 (2002) 841-859.
[59] T. Sadat-Shafai, J. Pucheault, C. Ferradini, A radiolysis study of the role of superoxide ion in the oxidation of sulfite by oxygen, Radiat. Phys. Chem. 17 (1981) 283-288.

Enhanced photocatalytic oxidation of SO_2 on TiO_2 surface by Na_2CO_3 modification

Haiming Wang[1,2], Changfu You[1,3]*, Zhongchao Tan[2,3]*

Highlights:

1. Photocatalytic oxidation of SO_2 on TiO_2 was improved after Na_2CO_3 modification
2. The improvement was due to the enhanced adsorption and photocatalytic ability
3. The recombination of electron-hole was suppressed by the formation of $CO_3^{\bullet-}$
4. The generation of hydroxyl radicals was promoted because of the deposited Na_2CO_3